International Journal of Thermal Sciences 49 (2010) 418–427

Contents lists available at ScienceDirect

International Journal of Thermal Sciences

journal homepage: www.elsevier.com/locate/ijts

Entropy generation analysis of electro-osmotic flow in open-end and closed-end micro-channels

L. Zhao, L.H. Liu*

School of Energy Science and Engineering, Harbin Institute of Technology, 92 West Dazhi Street, Harbin 150001, People's Republic of China

ARTICLE INFO

Article history:
Received 29 December 2008
Received in revised form
12 July 2009
Accepted 13 July 2009
Available online 30 July 2009

Keywords:
Volumetric entropy generation
Electro-osmotic flow
Joule heating
Viscous dissipation

ABSTRACT

The analysis of entropy generation mechanism is very important to optimize the second-law performance of these energy conversion devices in micro-scale. The entropy generation of electro-osmotic flow in two-dimensional open-end and closed-end micro-channels is analyzed and a rigorous mathematical model for describing electro-osmotic flow is used in this paper. The entropy generations of electro-osmotic flow due to heat conduction, viscous dissipation and Joule heating are numerically simulated. The results show that the volumetric entropy generation rates due to heat conduction and viscous dissipation exist the maximum value near the micro-channel wall, and the volumetric entropy generation rate due to Joule heating exists the maximum value at the center of the micro-channel. Because of the effect of Joule heating, the heat conduction entropy generation number and Joule heating entropy generation number increase with the applied electric field, and the entropy generation of viscous dissipation can be neglected in the open-end and closed-end electro-osmotic flow. When the temperature difference between the inlet and the top wall is larger than the temperature increment due to Joule heating, the electro-osmotic flow entropy generation due to heat conduction will take the major percent in the total entropy generation. When the temperature increment due to Joule heating is larger than the temperature difference between the inlet and the top wall, the electro-osmotic flow entropy generation due to Joule heating will take the major percent in the total entropy.

1. Introduction

During the last decade, the interest in the entropy generation minimization technique has experienced a huge growth for the thermal analysis of the flow systems in engineering devices [1,2]. Analysis of heat and fluid flow in micro-scale is of great importance not only for playing a key rule in the biological systems [3–5], but also for its application in cooling electronic equipment [6,7]. Understanding the flow and heat transfer in microscale is useful for the design [8,9], the fabrication and the operation of these micro-devices [10].

Some of the MEMS, such as micro-ducts, micro-nozzles, micro-pumps, micro-turbines and micro-valves, involve fluid flow. The micro-channels of micro-devices are defined as flow passages which have the hydraulic diameters in the range of 10 ~ 200 μm. The modeling of flow field in micro-channels should be predicted with a special attention to the effects of friction, roughness, rarefaction, compressibility, transition from laminar to turbulent, channel size, channel geometry and fluid type. The second law of thermodynamics has extensive application in problems involving heat transfer and fluid flow. Entropy generation is associated with thermodynamic irreversibility, which is present in all heat transfer and fluid flow processes. In the recently published paper, Erbay [11] analyzed the entropy generation in parallel plate micro-channels and got the conclusion that the entropy generation at the inlet and near the wall is larger, but no entropy is generated at the centerline of the duct for all values of group parameters. Hung [12] examined the viscous dissipation effect on entropy generation in a single-phase liquid flow in micro-channels. The results show that under certain conditions, the effect of viscous dissipation on entropy generation in micro-channel is significant and should not be neglected. Hooman [13] investigated the heat transfer and entropy generation for forced convection through a micro-duct of rectangular cross-section. Wang and Peng [14] and Peng et al. [15] have conducted an experimental investigation for a series of rectangular micro-channels to analyze the influence of liquid velocity, sub-cooling, property variations and micro-channel geometric configuration on the thermohydraulic characteristics. Their results show that all the parameters have significant influence on the heat transfer performance, cooling characteristics and liquid flow mode transition. Hetsroni et al. [16] discussed the

* Corresponding author. Tel.: +86 451 86402237.
E-mail address: lhliu@hit.edu.cn (L.H. Liu).

1290-0729/$ – see front matter © 2009 Elsevier Masson SAS. All rights reserved.
doi:10.1016/j.ijthermalsci.2009.07.009

Nomenclature

C_p	specific heat, J kg^{-1} K^{-1}
e	elementary charge, C
E	applied electric field intensity, V m^{-1}
H	height, m
k	thermal conductivity, W m^{-1} K^{-1}
k_b	Boltzmann constant, J K^{-1}
L	length, m
Ns	total entropy generation number
Ns_c	entropy generation number due to heat conduction
Ns_f	entropy generation number due to viscous dissipation
Ns_j	entropy generation number due to Joule heating
n_+	concentration of positive ion, m^{-3}
n_-	concentration of negative ion, m^{-3}
n_0	bulk concentration of ions, m^{-3}
p	pressure, Pa
P	dimensionless pressure
Q	total heat transfer rate of the system, W
Q_j	Joule heating, W m^{-3}
$\dot{S}'''_{gen,c}$	volumetric entropy generation rate due to heat conduction, W m^{-3} K^{-1}
$\dot{S}'''_{gen,f}$	volumetric entropy generation rate due to viscous dissipation, W m^{-3} K^{-1}
$\dot{S}'''_{gen,c}$	volumetric entropy generation rate due to Joule heating, W m^{-3} K^{-1}
S'''_{gen}	total heat transfer rate of the system, W m^{-3} K^{-1}
S^c_G	total entropy generation due to heat conduction, W K^{-1}
S^f_G	total entropy generation due to viscous dissipation, W K^{-1}
S^j_G	total entropy generation due to Joule heating, W K^{-1}
S_G	total entropy generation, W K^{-1}
T	temperature, K
u	axial velocity, m s^{-1}
u_s	Smoluchowski slip velocity, m s^{-1}
U	dimensionless axial velocity
x	axial coordinate
X	dimensionless axial coordinate
y	transverse coordinate
Y	dimensionless transverse coordinate
Z_+	valence of the positive ion
Z_-	valence of the negative ion
ε_r	dielectric constant of the fluid
ε_0	permittivity of vacuum, C V^{-1} m^{-1}
λ	electric conductivity of the fluid, m^{-1} S
λ_+	electric conductivity of n_+, $\cdot$m^2 S mol^{-1}
λ_-	electric conductivity of n_-, $\cdot$m^2 S mol^{-1}
η_+	mole concentration of cation in the electrolyte, mol/L
η_-	mole concentration of anion in the electrolyte, mol/L
μ	viscosity, Pa s
ρ	density, kg m^{-3}
ρ_e	net electric charge density, C m^{-3}
ψ	electrostatic potential, V
ς	zeta potential, V
$\dot{\gamma}$	viscosity dissipation source item

Subscripts

+	positive
−	negative

effect of viscous dissipation which may lead to drastic change of flow and temperature fields in micro-channels under certain conditions. It is validated from previous studies that the effect of viscous dissipation is significant in the first law analysis of fluid transport in micro-channels, in which the main concern is the flow and temperature distributions. Marco [17] researched how to implement a rigorous quantitative assessment of mixing quality in micro-fluidic devices. Xuan and Li [18] analyzed the electro-kinetic energy conversion. Hooman and Gurgenci [19] researched the influence of temperature-dependent viscosity on forced convection of a liquid through a parallel plate porous channel. The results show that the fully developed velocity and temperature differ substantially from constant property counterparts. Hooman et al. [20] studied the entropy generation for forced convection in a porous channel with isoflux or isothermal walls. Entropy generation for forced convection in a porous saturated circular tube and porous-saturated ducts of rectangular cross-section are investigated in Ref. [21,22]. Hung [23] systematically researched the viscous dissipation effect on entropy generation for non-Newtonian fluids in micro-channels.

To the best knowledge of the author, the systemic entropy analysis of electro-osmotic flow in the open-end and closed-end micro-channels has been reported rarely. In this paper, the local entropy generation of electro-osmotic flow due to heat conduction, viscous dissipation and Joule heating in the open-end and closed-end micro-channels are investigated. The effects of the applied electric field intensity and the temperature difference between the inlet and the top wall on the electro-osmotic flow entropy generation are studied respectively.

2. Mathematical formulae and method of simulation

Most surfaces acquire a certain amount of electrostatic charges when brought in contact with aqueous solutions [24]. The presence of such surface charges on the micro-channel surface will cause both counter-ions and co-ions in the liquid to be preferentially redistributed, leading to the formation of the electric double layer [25]. According to the electric double layer theory, the electrical potential in the diffuse part of the EDL is described by the Poisson equation, which is expressed as:

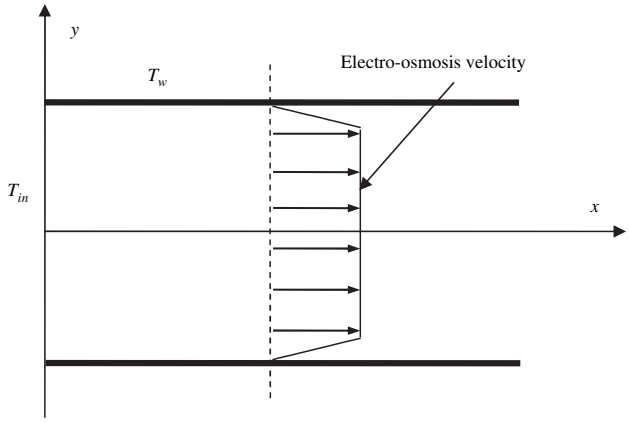

Fig. 1. Schematic of open-end micro-channel electro-osmotic flow.

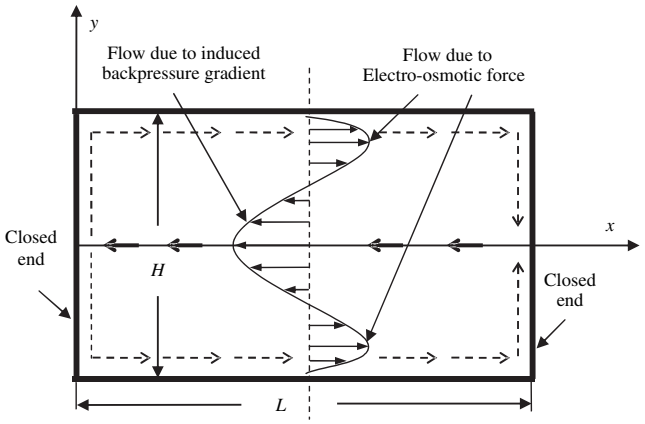

Fig. 2. Schematic of closed-end micro-channel electro-osmotic flow.

$$\frac{\partial}{\partial x_j}\left[\varepsilon_r \frac{\partial \psi}{\partial x_j}\right] = -\frac{\rho_e}{\varepsilon_0} \tag{1}$$

where ε_r is the dielectric constant of the electrolyte, ε_0 is the permittivity of vacuum, and ψ is the electrical potential of the EDL. The net charge density is given by

$$\rho_e = e(Z_+ n_+ + Z_- n_-) = -2|Z_\pm| e n_0 \sinh\left(\frac{|Z_\pm| e\psi}{k_b T}\right) \tag{2}$$

where Z is the valence of the ion, k_b is the Boltzmann constant, and e is the elementary charge.

In comparison to the flow driven by pressure, the electro-osmotic flow is driven by the applied electric field acting on the net ions in the diffuse part of the EDL. When an external electric field is applied along the streamwise direction, the ionized incompressible steady flow with electro-osmotic body forces is governed by the modified Navier–Stokes equations:

$$\frac{\partial(\rho u_j u_i)}{\partial x_j} = \frac{\partial}{\partial x_j}\left(\mu(T)\frac{\partial u_i}{\partial x_j}\right) - \frac{\partial p}{\partial x_i} + \rho_e E \tag{3}$$

where the liquid in micro-channel is NaCl electrolyte solution. The liquid density ρ is 998 kg/m^3, the liquid viscosity $\mu(T)$ is considered as a function of temperature expressed by $\mu(T) = 2.761 \times 10^{-6}\exp(1731/T)$ [26], and E is the applied electric field intensity.

Similar to Ref. [27], the effects of varying electric conductivity on the applied electric field strength and the Joule heating generated by the convection electric current are neglected in this paper. According to the Ohm's law, when considering Joule heating the modified energy equation is expressed as:

$$\frac{\partial(\rho C_p u_j T)}{\partial x_j} = \frac{\partial}{\partial x_j}\left(k(T)\frac{\partial T}{\partial x_j}\right) + \frac{1}{2}\mu\dot{\gamma}^2 + E^2 \cdot \lambda(T) \tag{4}$$

where the viscosity dissipation term is $|\overline{\gamma}| = \sqrt{[(\partial u_i/\partial x_j + \partial u_j/\partial x_i)^2 - 4/3(\partial u_k/\partial x_k)^2]}$ [28], the specific heat C_p is 4180.3 J/(kg K), and the thermal conductivity of the liquid $k(T)$ is considered as a function of temperature expressed by $k(T) = 0.6 + 2.5 \times 10^{-5}$ T [26].

The liquid electric conductivity is expressed as $\lambda = \lambda_+(T)\eta_+ + \lambda_-(T)\eta_-$, where the cation conductivity of the liquid $\lambda_+(T)$ is considered as a function of temperature expressed by $\lambda_+(T) = \lambda_{+0} + 7.453\lambda_{+0}(T/298.13 - 1)$, and the anion conductivity of liquid $\lambda_-(T)$ is similarly considered as a function of temperature expressed by $\lambda_-(T) = \lambda_{-0} + 7.453\lambda_{-0}(T/298.13 - 1)$. The cation electric conductivity at room temperature is $\lambda_{+0} = 50.08 \times 10^{-4}$ m^{2}S/mol, the anion electric conductivity at room temperature is $\lambda_{-0} = 76.31 \times 10^{-4}$ m^{2}S/mol [26]. η_+ and η_- respectively denote the mole concentration of cations and anions.

Figs. 1 and 2 show the schematic sketch of the physical situation, which consist of two parallel plates that are made of silicon glass exhibiting electro-osmotic effects and separated by a distance, H, and the length of the micro-channel is L. The micro-channel is filled with an ionized solution. The two closed-end walls are modeled as electrodes in the closed-end micro-channel and it is assumed that there is no EDL formation on the electrodes at the closed-end wall.

In a conventional electro-osmotic flow through an open-end micro-channel, the applied electric field interacting with the net ions in the diffuse layer of the EDL causes the liquid to move near the wall. Due to liquid viscosity, the movement of the ions will pull the liquid molecules along, leading to a plug-like velocity distribution at the developed condition. During electro-osmotic flow through a closed-end micro-channel, as the fluid layer at the EDL region flows towards the end of the channel where the fluid axial velocity becomes zero, the fluid gradually slows down and thus induces a pressure distribution in the channel. This causes the fluid to move in the radial direction towards the center region of the channel and flow through the center core of the cross-section area to ensure zero net flow, which result in two circulating flows in the whole closed-end micro-channel. Fig. 2 presents the overall schematic of an electro-osmotic flow through a closed-end micro-

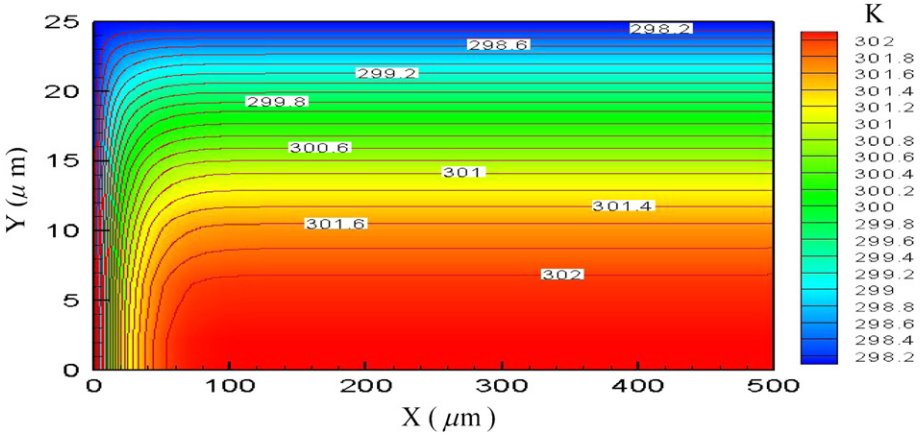

Fig. 3. Temperature distribution in the open-end micro-channel.

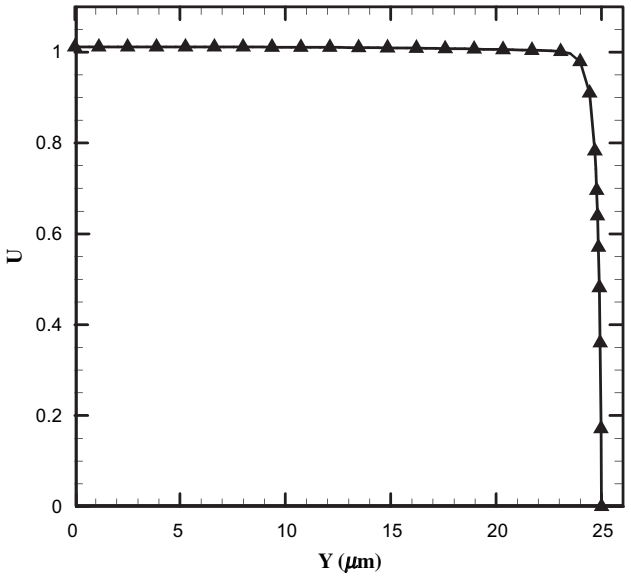

Fig. 4. Dimensionless velocity distribution at the central of the open-end micro-channel.

channel. The velocity profile of the flow in the fully developed region is also shown in Fig. 2, where the two peaks of the flow near the wall are due to the electro-osmotic force and the flow at the center core region is due to the induced backpressure.

As shown in Figs. 1 and 2, due to symmetry only the top half of the geometry is modeled. The boundary condition for electro-osmotic flow in the closed-end micro-channel is specified below:

$$\text{at } x = 0: \; u = 0,\; v = 0,\; \frac{\partial \psi}{\partial x} = 0,\; T_{\text{in}} = 298\ \text{K};$$

$$\text{at } x = L: \; u = 0,\; v = 0,\; \frac{\partial \psi}{\partial x} = 0,\; T_{\text{out}} = 298\ \text{K};$$

$$\text{at } y = 0: \; \frac{\partial u}{\partial y} = 0,\; v = 0,\; \frac{\partial \psi}{\partial y} = 0,\; \frac{\partial T}{\partial y} = 0;$$

$$\text{at } y = \frac{H}{2}: \; u = 0,\; v = 0,\; \psi = \zeta,\; T_w = 298\ \text{K}$$

Similarly, the boundary condition for electro-osmotic flow in the open-end micro-channel is specified below:

$$\text{at } x = 0: \; \frac{\partial u}{\partial x} = 0,\; v = 0,\; \psi = 0,\; T_{\text{in}} = 298\ \text{K};$$

$$\text{at } x = L: \; \frac{\partial u}{\partial x} = 0,\; \frac{\partial v}{\partial x} = 0,\; \frac{\partial \psi}{\partial x} = 0,\; \frac{\partial T}{\partial x} = 0;$$

$$\text{at } y = 0: \; \frac{\partial u}{\partial y} = 0,\; v = 0,\; \frac{\partial \psi}{\partial y} = 0,\; \frac{\partial T}{\partial y} = 0;$$

$$\text{at } y = \frac{H}{2}: \; u = 0,\; v = 0,\; \psi = \zeta,\; T_w = 298\ \text{K}$$

Generally speaking, the electro-osmotic flow in the micro-channel is laminar, according to the method adopted in Ref. [29], the local volumetric entropy generation rate due to heat conduction is determined as:

$$S'''_{\text{gen},c} = \frac{k}{T^2}(\nabla T)^2 \tag{5}$$

where k is the thermal conductivity of the liquid, and T is the local temperature. The local volumetric entropy generation rate due to viscous dissipation is defined as:

$$S'''_{\text{gen},f} = \frac{\mu}{T}\left\{2\left[\left(\frac{\partial u}{\partial x}\right)^2 + \left(\frac{\partial v}{\partial y}\right)^2\right] + \left(\frac{\partial v}{\partial y} + \frac{\partial u}{\partial x}\right)^2\right\} \tag{6}$$

where μ is the viscosity of the liquid. The local volumetric entropy generation rate due to Joule heating is described as:

$$S'''_{\text{gen},j} = \frac{Q_j}{T} \tag{7}$$

where $Q_j = E^2 \cdot \lambda(T)$ is the Joule heating. The volumetric entropy generation rate per unit volume in the micro-channel can be written as:

$$S'''_{\text{gen}} = S'''_{\text{gen},c} + S'''_{\text{gen},f} + S'''_{\text{gen},j} \tag{8}$$

The total entropy generation due to the heat conduction, viscous dissipation and Joule heating can be derived by integrating Eqs. (5)–(7) over volume as follows:

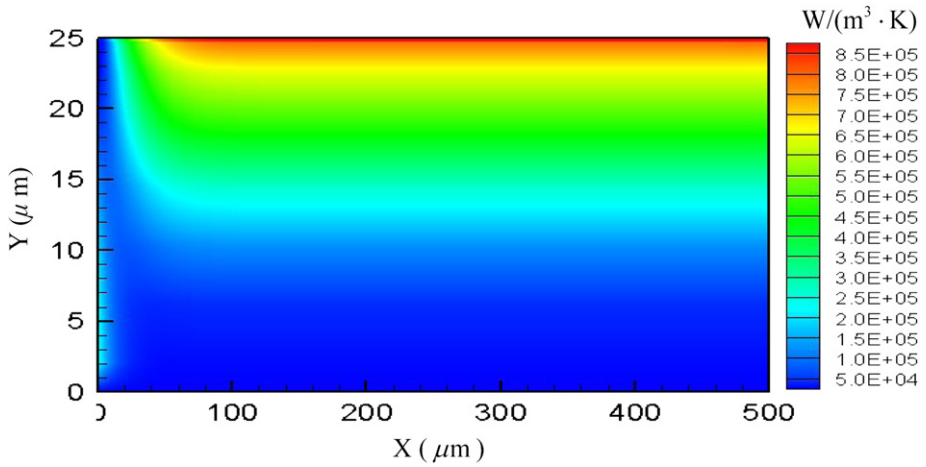

Fig. 5. Distribution of the volumetric entropy generation rate due to heat conduction in the open-end micro-channel.

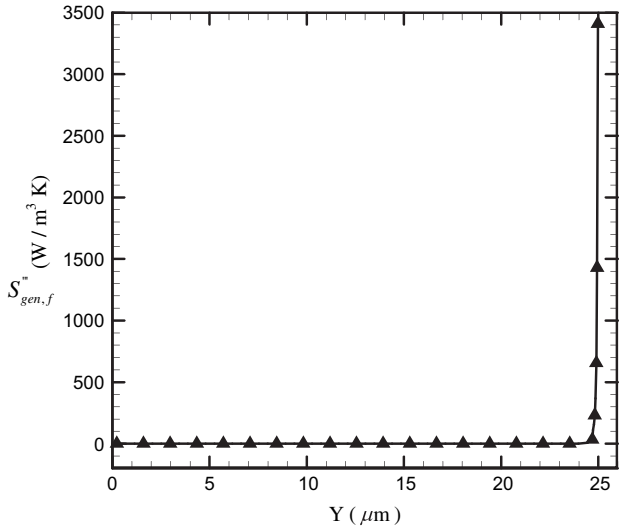

Fig. 6. Distribution of the volumetric entropy generation rate due to viscous dissipation at the central region of open-end micro-channel.

$$S_G^c = \int_V S'''_{\mathrm{gen},c}\,dV \tag{9}$$

$$S_G^f = \int_V S'''_{\mathrm{gen},f}\,dV \tag{10}$$

$$S_G^j = \int_V S'''_{\mathrm{gen},j}\,dV \tag{11}$$

The total entropy generation in the micro-channel considering here is

$$S_G = S_G^c + S_G^f + S_G^j \tag{12}$$

The entropy generation number is often used to evaluate the irreversibility of the process in the second law analysis of heat transfer and flow processes. In the following analysis, the entropy generation numbers of the electro-osmotic flow due to heat conduction, viscous dissipation and Joule heating are defined respectively as:

Table 1
The entropy generation of electro-kinetic flow under different micro-channel heights and ratios of micro-channel length and height in the open-end micro-channel.

L/H	H = 25 μm			H = 50 μm		
	S_G^c(W K^{-1})	S_G^j(W K^{-1})	S_G^f(W K^{-1})	S_G^c(W K^{-1})	S_G^j(W K^{-1})	S_G^f(W K^{-1})
10	1.1×10^{-3}	5.7×10^{-6}	1.4×10^{-5}	9.9×10^{-3}	7.5×10^{-4}	2.0×10^{-6}
100	4.6×10^{-2}	1.9×10^{-3}	2.0×10^{-5}	1.9×10^{-1}	3.2×10^{-2}	8.8×10^{-6}

$$Ns_c = \frac{S_G^c T_0}{Q} \tag{13}$$

$$Ns_f = \frac{S_G^f T_0}{Q} \tag{14}$$

$$Ns_j = \frac{S_G^j T_0}{Q} \tag{15}$$

where Q is the total heat transfer rate of the system, which is calculated by the heat transfer rates of the top wall, the bottom wall, the inlet region and the outlet region of the micro-channel. The total entropy generation number of the system can be written as:

$$Ns = Ns_c + Ns_f + Ns_j = \frac{S_G T_0}{Q} \tag{16}$$

The numerical solutions to equations (1)–(4) subject to the above boundary conditions were obtained based on a control-volume method detailed by Patankar [30] using FORTRAN language. In this procedure, the domain was discretized by a series of control volumes, each containing a grid point. The differential equation was expressed in an integral form over the control volume, leading to a system of algebraic equations that could be solved in an iterative manner. Pressure–velocity coupling was handled by the SIMPLER formulation as described by Patankar [30]. The computation began with guessing the pressure field and solving the momentum equations to obtain the velocity field. The continuity equation was then used to obtain the corrected pressure field, which was used as a new guess. A grid-independent test is carried out to ensure that the chosen grid system can produce grid-independent solutions.

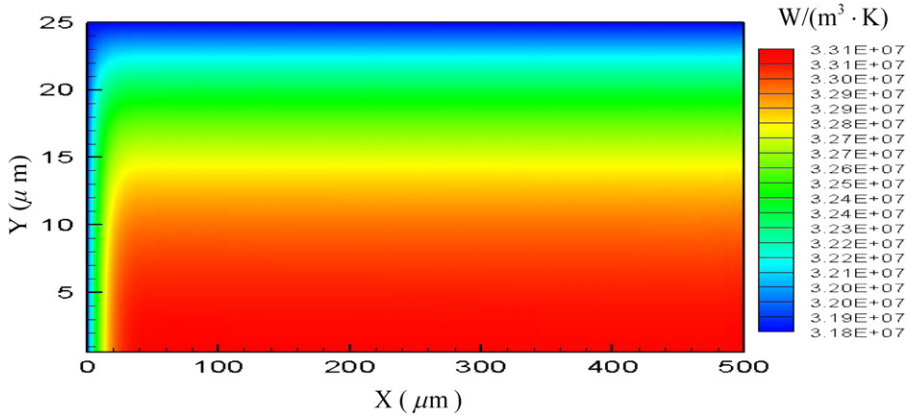

Fig. 7. Distribution of the volumetric entropy generation rate due to Joule heating in the open-end micro-channel.

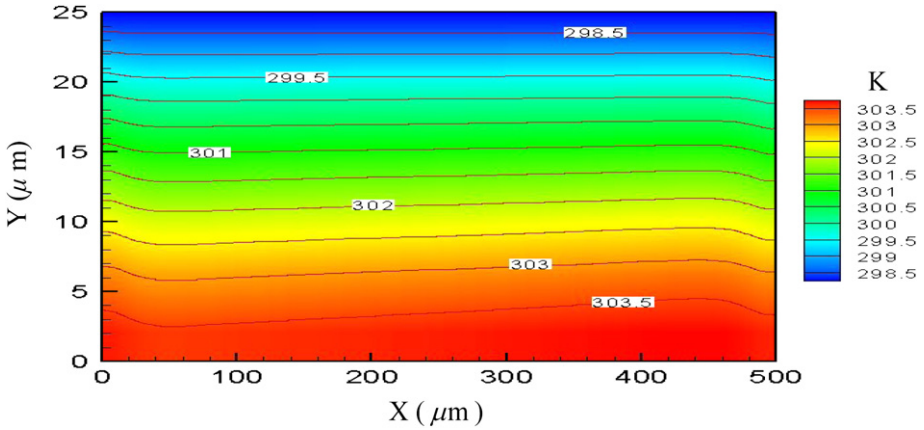

Fig. 8. Temperature distribution in the closed-end micro-channel.

3. Results and discussion

3.1. Volumetric entropy generation rate distribution of electro-osmotic flow in open-end micro-channel

This part of paper researches the local volumetric entropy generation rates of heat conduction, viscous dissipation and Joule heating in the open-end electro-osmotic flow. The applied electric field is 500 V/cm, zeta potential ς is 150 mV, the ion concentration is 10^{-3} μm, the dielectric constant of the electrolyte ε_0 is 8.85419×10^{-12} C V^{-1} m^{-1}, the permittivity of vacuum ε_r is 79, the micro-channel height is $H = 50$ μm, and the micro-channel length is $L = 500$ μm. The dimensionless form of the variable $U = u/u_s$ is used to present the results. Here, u_s is the Smoluchowski slip velocity [31] defined as $u_s = \varepsilon_r \varepsilon_0 \varsigma E/\mu$. The Smoluchowski slip velocity is 5.87×10^{-3} m/s in this paper.

The temperature and velocity distributions of electro-kinetic flow in the open-end micro-channel are shown in Figs. 3 and 4. The local volumetric entropy generation rate distributions due to heat conduction and viscous dissipation in the open-end electro-osmotic flow are shown in Figs. 5 and 6 respectively. The local volumetric entropy generation rate due to heat conduction depends on the temperature gradient in the micro-channel, while the volumetric entropy generation rate due to viscous dissipation is relative to the velocity gradient. The Joule heating is a volumetric heat and increases with the ions concentration increment, as shown in Fig. 3, the highest temperature occurs at the centerline which suggests that the heat generated by Joule heating is transferred from the central region to the wall by convective. But the highest fluid temperature gradient appears near the wall. Thus, Fig. 5 shows that the maximum volumetric entropy generation rate due to heat conduction is near the wall and the smallest volumetric entropy generation rate due to heat conduction occurs in the central region of the micro-channel.

It is known that the electro-osmotic flow in the micro-channel is plug-like as shown in Fig. 4. Therefore, the velocity varies rapidly from zero to the maximum velocity in the region of electric double layer, and the velocity gradient is very large near the wall. Because of the plug-like velocity distribution, the velocity gradient in the central part of the micro-channel is nearly zero. The entropy generation of viscous dissipation is relative to the velocity gradient. Accordingly, Fig. 6 presents that the maximum volumetric entropy generation rate due to viscous dissipation locates near the wall and the volumetric entropy generation rate due to viscous dissipation is nearly zero at the central region of the micro-channel.

The local electro-osmotic flow volumetric entropy generation rate distribution due to Joule heating is shown in Fig. 7. The maximum entropy rate of Joule heating appears at the center of the micro-channel. The reason is that the Joule heating makes the highest temperature existing at the center of the micro-channel which results in a larger electric conductivity of the fluid according to Section 2.

Table 1 shows that the entropy generation of electro-kinetic flow under different micro-channel heights and ratios of micro-channel length and height in the open-end micro-channel. As shown in Table 1, the electro-osmotic flow entropy generation due to viscous dissipation can be omitted in the open-end micro-channel.

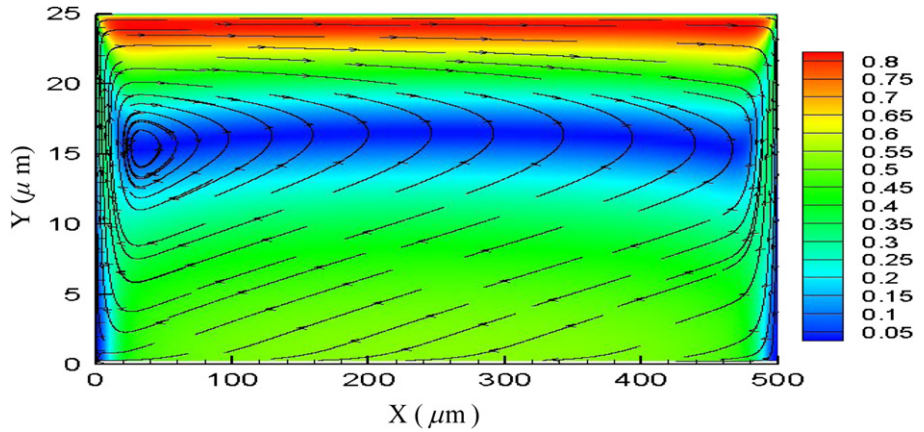

Fig. 9. Dimensionless velocity distribution in the closed-end micro-channel.

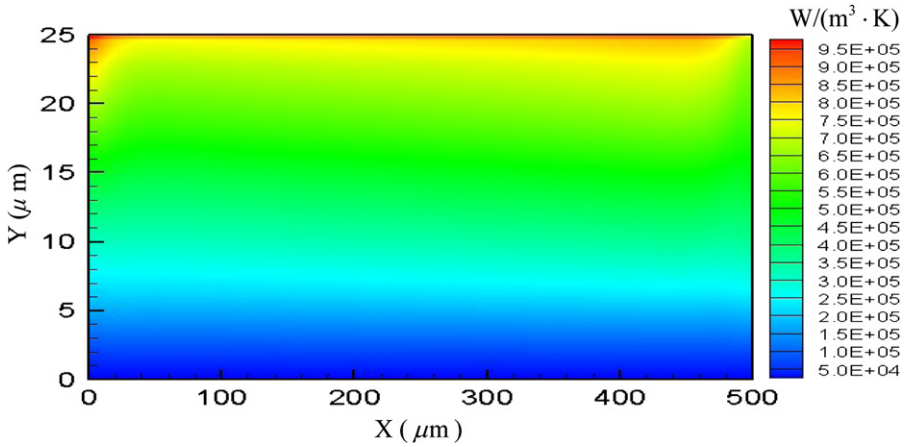

Fig. 10. Distribution of the volumetric entropy generation rate due to heat conduction in the closed-end micro-channel.

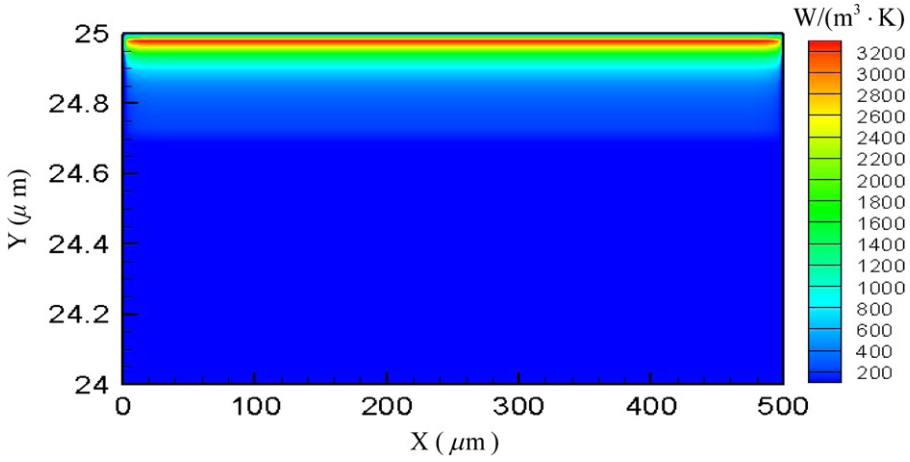

Fig. 11. Distribution of the volumetric entropy generation rate due to viscous dissipation in the closed-end micro-channel.

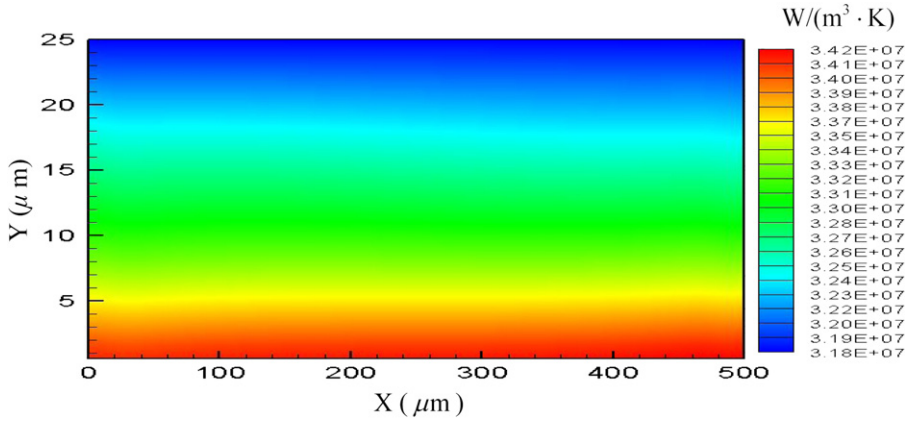

Fig. 12. Distribution of the volumetric entropy generation rate due to Joule heating in the close-end micro-channel.

3.2. Volumetric entropy generation distribution of electro-osmotic flow in closed-end micro-channel

The electro-osmotic flow volumetric entropy generation rate distribution in the closed-end micro-channel is different from that in the open-end micro-channel due to the circulating flow characteristic of the closed-end electro-osmotic flow. The same parameters as mentioned in Section 3.1 are used in the closed-end electro-osmotic flow. The electro-osmotic flow velocity and the temperature fields in the closed-end micro-channel are shown in Figs. 8 and 9, respectively. The volumetric entropy generation rate distribution due to heat conduction and that due to viscous dissipation are shown in Figs. 10 and 11, respectively. Fig. 8 presents that the highest temperature occurs at the central part of the micro-channel and the maximum temperature gradient exists near the wall. The temperature distribution, being not homogeneous like that in the open-end electro-osmotic flow, looks like flat S-shaped due to the circulating flow characteristic of the closed-end electro-

Table 2
The entropy generation of electro-kinetic flow under different micro-channel heights and ratios of micro-channel length and height in the closed-end micro-channel.

L/H	$H = 25\ \mu m$			$H = 50\ \mu m$		
	$S_G^c(W K^{-1})$	$S_G^j(W K^{-1})$	$S_G^f(W K^{-1})$	$S_G^c(W K^{-1})$	$S_G^j(W K^{-1})$	$S_G^f(W K^{-1})$
10	3.5×10^{-2}	5.5×10^{-5}	3.9×10^{-6}	2.2×10^{-2}	1.7×10^{-3}	1.0×10^{-6}
100	2.1×10^{-1}	7.0×10^{-3}	2.3×10^{-5}	4.0×10^{-1}	5.6×10^{-2}	1.1×10^{-5}

osmotic flow. Thus, the volumetric entropy generation rate due to heat conduction varies acutely near the wall and also looks like flat S=shaped as shown in Fig. 9. The velocity distribution in the whole micro-channel appears wave-like shape. Because we just simulate the top half part of the micro-channel, there is only one circulating flow as shown in Fig. 10. The velocity of electro-osmotic flow in the closed-end micro-channel varies acutely near the wall, so the maximum volumetric entropy generation rate due to viscous dissipation locates near the wall as shown in Fig. 11. Because of the negative flow at the central part of the micro-channel, there is a larger velocity gradient at the central part of the micro-channel, which differs from that in the open-end electro-osmotic flow, in which the velocity gradient at the central part of the micro-channel is nearly zero. Thus, the entropy generation at the core region of the micro-channel due to viscous dissipation in the closed-end micro-channel electro-osmotic flow is larger than that in the open-end micro-channel electro-osmotic flow.

Fig. 12 shows the local volumetric entropy generation rate distribution due to Joule heating. The maximum volumetric entropy generation rate of Joule heating occurs at the center region of the micro-channel. The reason is that the Joule heating causes the maximum temperature existing at the center of the micro-channel which results in a larger electric conductivity of the fluid according to Section 2. The electro-osmotic flow entropy generation distribution of Joule heating in the closed-end micro-channel looks more uniform comparing with that in the open-end micro-channel due to the circulating flow characteristic of closed-end electro-osmotic flow.

Table 2 shows that the entropy generation of electro-kinetic flow under different micro-channel heights and ratios of micro-channel length and height in the closed-end micro-channel. It is same with the case in the open-end micro-channel electro-osmotic flow. As shown in Table 2, the entropy generation of electro-osmotic flow due to viscous dissipation can also be omitted in the closed-end electro-osmotic flow under different micro-channel heights and ratios of micro-channel length and height.

3.3. Entropy generation of electro-osmotic flow for different temperature difference

In order to research the relation between the electro-osmotic flow entropy generations of heat conduction and Joule heating, we need to do some further research. Firstly, we research the effect of the temperature difference between the inlet and the top wall on the electro-osmotic flow entropy generation of heat conduction and Joule heating when the applied electric field is 10V/cm. Secondly, we research the effect of the applied electric field on the electro-osmotic flow entropy generation due to heat conduction and Joule heating when temperature difference between the inlet and the top wall is 5 K. The inlet temperature for a closed-end micro-channel is the left wall temperature. The following part of the paper analyses the entropy generation of electro-osmotic flow for different applied electric fields and temperature differences in the open-end and closed-end micro-channel. The ratio of the micro-channel length to height is kept constant, i.e. $L : H = 10 : 1$ in order to compare different situations in the following calculations [32].

Table 3
Apportioning of total entropy generation of electro-kinetic flow and their percents for different temperature difference between inlet temperature and top wall temperature in the open-end micro-channel when the applied electric field is 10 V/m.

ΔT(K)	S_G^c/S_G	S_G^f/S_G	S_G^j/S_G	$S_G(W K^{-1})$	Ns
1	23%	0%	77%	2.06×10^{-4}	1.66×10^{-2}
5	87.3%	0%	12.7%	1.33×10^{-3}	1.74×10^{-2}
10	96.2%	0%	3.82%	4.73×10^{-3}	3.09×10^{-2}
30	99.4%	0%	0.6%	3.77×10^{-2}	8.20×10^{-2}
60	99.8%	0%	0.2%	1.33×10^{-1}	1.44×10^{-1}

Table 4
Apportioning of total entropy generation of electro-kinetic flow and their percents for different temperature difference between left wall temperature and top wall temperature in the closed-end micro-channel when the applied electric field is 10 V/m.

ΔT(K)	S_G^c/S_G	S_G^f/S_G	S_G^j/S_G	$S_G(W K^{-1})$	Ns
0	0.2%	0%	99.8%	1.57×10^{-4}	1.20×10^{-1}
1	12.8%	0%	87.2%	1.83×10^{-4}	1.31×10^{-2}
5	77.8%	0%	22.2%	7.66×10^{-4}	1.01×10^{-2}
10	92.8%	0%	7.24%	2.51×10^{-3}	1.65×10^{-2}
30	98.8%	0%	1.19%	1.92×10^{-2}	4.19×10^{-2}
60	99.6%	0%	0.4%	6.58×10^{-2}	7.16×10^{-2}

Tables 3 and 4 show the electro-osmotic flow entropy generations of heat conduction, viscous dissipation and Joule heating and their proportions in the total entropy generation in the open-end and closed-end micro-channel for different temperature difference between the inlet and the top wall when the applied electric field is 10 V/cm. The electro-osmotic flow entropy generation of heat conduction takes the dominant effect both in open-end and closed-end electro-osmosis when the temperature difference is large. But the electro-osmotic flow entropy generation of Joule heating takes the major percent in the total entropy generation when the temperature difference is small. The electro-osmotic flow entropy generation due to viscous dissipation can be neglected both in open-end and closed-end micro-channel. For the same parameter, the percent of heat conduction entropy generation in total entropy generation in the closed-end micro-channel is smaller than that in

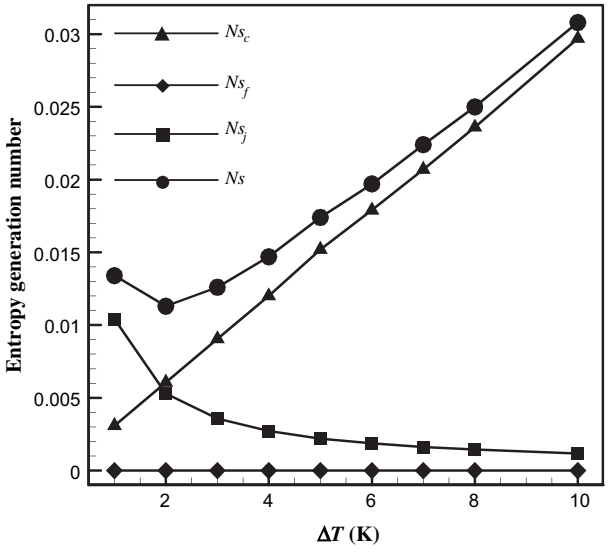

Fig. 13. Effect of the temperature difference between inlet temperature and top wall temperature on electro-osmotic flow entropy generation number in the open-end micro-channel when the applied electric field is 10 V/cm.

Table 5
Apportioning of total entropy generation of electro-kinetic flow and their percents for different applied electric field in the open-end micro-channel when the temperature difference between inlet temperature and top wall temperature is 5 K.

E(V/cm)	S_G^c/S_G	S_G^f/S_G	S_G^j/S_G	S_G(W K^{-1})	Ns
10	87.3%	0%	12.7%	1.33×10^{-3}	1.74×10^{-2}
50	21.4%	0%	78.6%	5.37×10^{-3}	7.09×10^{-2}
100	6.14%	0%	93.9%	1.80×10^{-2}	2.46×10^{-1}
300	0.51%	0%	99.5%	1.53×10^{-1}	3.38×10^{0}
500	0.16%	0%	99.8%	4.34×10^{-1}	4.72×10^{1}

the open-end micro-channel. It is because that the circulating flow characteristic of the closed-end electro-osmotic flow makes the fluid temperature to be homogeneous which leads to a smaller heat transfer rate of the system.

Fig. 13 presents electro-osmotic flow entropy generation numbers of heat conduction, viscous dissipation and Joule heating varying with the temperature difference between the inlet and the top wall. The heat conduction entropy generation number increases with the temperature difference increasing in both the open-end and the closed-end electro-osmotic flow. The Joule heating entropy generation number decreases with the temperature difference increasing in the open-end and the closed-end electro-osmotic flow. When the temperature difference between inlet temperature and top wall temperature is small, the Joule heating entropy generation number is larger than the heat conduction entropy generation number. When the temperature difference between inlet temperature and top wall temperature is large, the heat conduction entropy generation number is larger than the Joule heating entropy number. It means that the heat conduction becomes the main modes of heat transfer.

3.4. Entropy generation of electro-osmotic flow for different applied electric fields

Tables 5 and 6 show the electro-osmotic flow entropy generations of heat conduction, viscous dissipation and Joule heating and their proportion in the total entropy generation in the open-end and closed-end micro-channel for different applied electric fields when the temperature difference between inlet and top wall is 5 K. The electro-osmotic flow entropy generation of heat conduction takes the major percent in the total entropy generation both in open-end and closed-end electro-osmotic flow when applied electric field is small. The electro-osmotic flow entropy generation number of Joule heating takes the major percent in the total entropy generation when the applied electric field is large. The entropy generation of electro-osmotic flow due to viscous dissipation can be neglected. For the same parameter, the percent of heat conduction entropy generation in total entropy generation in the closed-end micro-channel is smaller than that in the open-end micro-channel due to circulating flow characteristic of the closed-end electro-osmotic flow.

Fig. 14 presents the electro-osmotic flow entropy generation numbers of heat conduction, viscous dissipation and Joule heating varying with the applied electric field when the temperature difference between inlet and top wall is 5 K. The heat conduction entropy number varies small with the applied electric field, and the Joule heating entropy generation number increases with the applied electric field increasing. The reason is that the fluid temperature increment due to Joule heating is small comparing to the temperature difference between the inlet temperature and the top wall temperature.

Table 6
Apportioning of total entropy generation of electro-kinetic flow and their percents for different applied electric field in the closed-end micro-channel when the temperature difference between left wall temperature and top wall temperature is 5 K.

E(V/cm)	S_G^c/S_G	S_G^f/S_G	S_G^j/S_G	S_G(W K^{-1})	Ns_j
10	77.8%	0%	22.2%	7.66×10^{-4}	1.02×10^{-2}
50	11.6%	0%	88.4%	4.81×10^{-3}	6.97×10^{-2}
100	2.88%	0%	97.1%	1.75×10^{-2}	2.94×10^{-1}
300	0.21%	0%	99.8%	1.55×10^{-1}	2.73×10^{1}
500	0.17%	0%	99.8%	4.39×10^{-1}	5.80×10^{2}

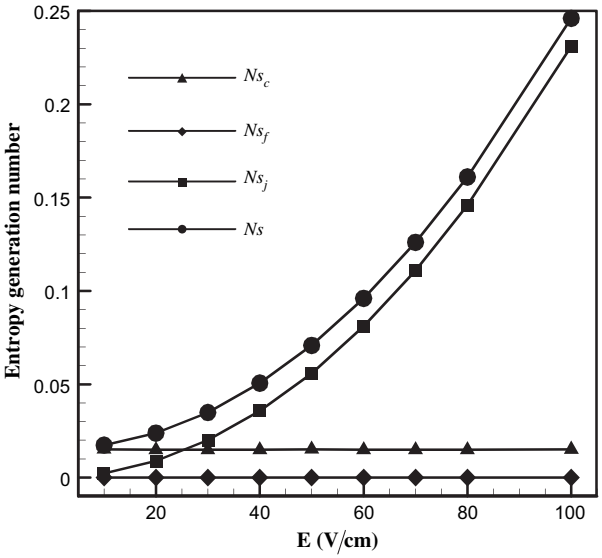

Fig. 14. Effect of the applied electric field on electro-osmotic flow entropy generation number in the open-end micro-channel when the temperature difference between inlet temperature and top wall temperature is 5 K.

4. Conclusions

Entropy generation is associated with thermodynamic irreversibility, which is present in all heat transfer and fluid flow processes. In this paper, we studied the entropy generation of electro-osmotic flow in the two-dimensional open-end and closed-end micro-channel. The main conclusions from present analysis can be summarized that the volumetric entropy generation rates due to heat conduction and viscous dissipation exist the maximum value near the wall, and the maximum volumetric entropy generation rate due to Joule heating appears at the center of the micro-channel. The electro-osmosis flow entropy generation of viscous dissipation can be neglected in the open-end and closed-end micro-channel. For the same parameter, the percent of the electro-osmotic flow entropy generation due to heat conduction in the total entropy generation in closed-end micro-channel is smaller than that in open-end micro-channel due to the circulating flow characteristic of the closed-end electro-osmotic flow. When the fluid temperature increment due to Joule heating is larger than the temperature difference between inlet and top wall, the percent of electro-osmotic flow entropy generation due to Joule heating in the total entropy generation is larger. When the fluid temperature increment due to Joule heating is smaller than the temperature difference between inlet and top wall, the heat conduction entropy generation of electro-osmotic flow will take the major percent in the total entropy generation.

Acknowledgements

The support of this work by the Changjiang Scholars and Innovative Research Team in University (IRT0520) and the

Inter-discipline Crossed Foundation of Harbin Institute of Technology (HIT.MD200320) is gratefully acknowledged.

References

[1] Y. Azoumah, P. Neveu, N. Mazet, Constructal design combined with entropy generation minimization for solid–gas reactors, International Journal of Thermal Sciences 45 (2006) 716–728.
[2] H. Abbassi, Entropy generation analysis in a uniformly heated microchannel heat sink, Energy 32 (2007) 1932–1947.
[3] G.L. Morini, Scaling effects for liquid flows in microchannels, Heat Transfer Engineering 27 (4) (2006) 64–73.
[4] K. Hooman, Entropy generation for microscale forced convection: effects of different thermal boundary conditions, velocity slip, temperature jump, viscous dissipation, and duct geometry, International Communications in Heat and Mass Transfer 34 (8) (2007) 945–957.
[5] S. Mahmud, R.A. Fraser, Flow, thermal, and entropy generation characteristics inside a porous channel with viscous dissipation, International Journal of Thermal Sciences 44 (2005) 21–32.
[6] A. Bejan, Entropy Generation Minimization, CRC Press, New York, 1996.
[7] A. Bejan, Entropy Generation through Heat and Fluid Flow, Wiley, Canada, 1994.
[8] J.L. Xu, Y.H. Gan, Oscillating flow behavior of a natural circulation loop using minichannels at atmospheric pressure, Applied Thermal Engineering 24 (2004) 2665–2677.
[9] G.S. Zhang, W. Du, B.F. Liu, et al., Characterization of electrokinetic gating valve in microfluidic channels, Analytica Chimica Acta 584 (2007) 129–135.
[10] C. Ye, D.Q. Li, Electrophoretic motion of two spherical particles in a rectangular microchannel, Microfluid Nanofluid 1 (2004) 52–61.
[11] L.B. Erbay, M.M. Yalcin, M.S. Ercan, Entropy generation in parallel plate microchannels, Heat Mass Transfer 43 (2007) 729–739.
[12] Y.M. Hung, A comparative study of viscous dissipation effect on entropy generation in single-phase liquid flow in microchannels, International Journal of Thermal Sciences 48 (2009) 1026–1035.
[13] K. Hooman, Heat transfer and entropy generation for forced convection through a microduct of rectangular cross-section: effects of velocity slip, temperature jump, and duct geometry, International Communications in Heat and Mass Transfer 48 (2008) 1065–1068.
[14] B.X. Wang, X.F. Peng, Experimental investigation on liquid forced-convection heat transfer through microchannels, International Journal of Heat and Mass Transfer 37 (1994) 73–82.
[15] X.F. Peng, B.X. Wang, G.P. Peterson, H.B. Ma, Experimental investigation of heat transfer in flat plates with rectangular microchannels, International Journal of Heat and Mass Transfer 38 (1995) 127–137.
[16] G. Hetsroni, A. Mosyak, E. Pogrebnyak, L.P. Yarin, Heat transfer in microchannels: comparison of experiments with theory and numerical results, International Journal of Heat and Mass Transfer 48 (2005) 5580–5601.
[17] C. Marco, M.Z. Ica, K. Miron, Entropic characterization of mixing in microchannels, Journal of Micromechanicsand Microengineering 15 (2005) 2038–2044.
[18] X.C. Xuan, D.Q. Li, Thermodynamic analysis of electrokinetic energy conversion, Journal of Power Sources 156 (2006) 677–684.
[19] K. Hooman, H. Gurgenci, Effects of temperature-dependent viscosity on forced convection inside a porous medium, Transport in Porous Media 75 (2008) 249–267.
[20] K. Hooman, F. Hooman, S.R. Mohebpour, Entropy generation for forced convection in a porous channel with isoflux or isothermal walls, International Journal of Exergy 5 (2008) 78–96.
[21] K. Hooman, H. Gurgenci, A.A. Merrikh, Heat transfer and entropy generation optimization of forced convection in porous-saturated ducts of rectangular cross-section, International Journal of Heat and Mass Transfer 50 (2007) 2051–2059.
[22] K. Hooman, A. Ejlali, Entropy generation for forced convection in a porous saturated circular tube with uniform wall temperature, International Communications in Heat and Mass Transfer 34 (2007) 408–419.
[23] Y.M. Hung, Viscous dissipation effect on entropy generation for non-Newtonian fluids in microchannels, International Communications in Heat and Mass Transfer 35 (2008) 1125–1129.
[24] R.J. Hunter, Zeta Potential in Colloid Science: Principles and Applications, Academic Press, New York, 1981.
[25] G.M. Mala, D.Q. Li, G. Werner, H.J. Jacobasch, Y.B. Ning, Flow characteristics of water through a microchannel between two parallel plates with electrokinetic effects, International Journal of Heat Fluid Flow 18 (1997) 489–496.
[26] R. Weast, M.J. Astle, W.H. Beyer, CRC Handbook of Chemistry and Physics, CRC Press Inc, Boca Raton, 1986.
[27] G.Y. Tang, C. Yang, J.C. Chai, H.Q. Gong, Joule heating effect on electroosmotic flow and mass species transport in a microcapillary, International Journal of Heat and Mass Transfer 47 (2004) 215–227.
[28] X.Y. Chen, K.C. Toh, C. Yang, J.C. Chai, Numerical computation of hydrodynamically and thermally developing liquid flow in microchannels with electrokinetics effects, Journal of Heat Transfer 126 (2004) 70–75.
[29] H. Yapaci, N. Kayatas, B. Albayrak, G. Basturk, Numerical calculation of local entropy generation in a methane–air burner, Energy Conversion and Management 46 (2005) 1885–1919.
[30] S.V. Patankar, Numerical Heat Transfer and Fluid Flow, Hemisphere, Washington DC, 1980.
[31] R.F. Probstein, Physicochemical Hydrodynamics: An Introduction, John Wiley and Sons, New York, 1994.
[32] K.T. Marcos, C. Ooi, J.C. YangChai, T.N. Wong, Developing electro-osmotic flow in closed-end micro-channels, International Journal of Engineering Science 43 (2005) 1349–1362.